Optics & Spectroscopy, 2004, 96 (6): 946-951

Spatial Localization of Biosensor Fluorescence Signals in Human Skin under the Effect of Equalization of the Refractive Index of the Surrounding Medium

I. V. Meglinski and D. Y. Churmakov

Cranfield University, School of Engineering, Cranfield, MK43 0AL, UK

E-mail: i.meglinski@cranfield.ac.uk

Abstract—A priority line of biomedical applications of optics is the development of noninvasive diagnostic methods based on the scanning of fluorescence radiation of biosensors embedded in biological tissue. Their main advantage is a high sensitivity and selectivity with respect to given parameters of tissues and their variations. In this study, we present a method for and results of modeling of excitation and propagation of fluorescence radiation in a multilayer randomly inhomogeneous highly scattering and absorbing medium imitating human skin. The model takes into account the spatially inhomogeneous distribution of skin fluorophores and their photophysical characteristics. Both the spatial distribution of fluorescence of skin tissues and the possibility of localization of a detected fluorescence signal are studied. The spatial distribution of fluorescence centers (fluorophores) in the medium is assumed to closely follow the spatial distribution of collagen fibers of the skin. The equalization of the refractive indices at the air–skin interface is shown to lead to a higher degree of localization of the fluorescence signal detected from a biosensor located in a near-surface skin layer.

1. INTRODUCTION

Recently, considerable attention has been focused on the development of nano- and optical technologies because of the unique possibility of their use in numerous practical applications, including various areas of biology and medicine [1]. Advances that have been made in optics, biophysics, biochemistry, and microelectronics allow the creation of miniature devices operating as biosensors [2, 3]. Although these artificial biosensors allow one to measure fairly accurately various biochemical and biophysical characteristics of biological tissues, they still have limited applications. First of all, this is explained by the difficulties arising upon implantation of elements of an artificial sensor in living tissues and by the problem of communication between the sensor and a detector.

In the context of the solution of these problems and further development of clinical methods of rapid diagnostics and noninvasive monitoring (dynamic observation) of the state of health, a method of scanning of a fluorescence signal emitted by a fluorescing sensor (or group of sensors) placed at a specified depth in human skin was proposed [4]. As a possible method of incorporation of biosensors, the use of children's nonpermanent (washable) tattoos applied to the skin surface has been suggested. The composition of the tattoo paint involves matrix biopolymers with specified fluorescent characteristics, which vary depending on physiological changes caused by variations in the skin temperature; concentrations of oxygen, hemoglobin, and glucose; medicinal preparations; and so on.

The main advantage of this method is the fundamental possibility of spatial localization of a detected optical signal within a small controlled volume. However, in order to choose the optimal configuration of the measuring scanning system and to enable the subsequent quantitative interpretation of the fluorescence signal detected, a detailed analysis of the effective region of measurements is necessary. This, in turn, implies the construction of an adequate model of the fluorescence of biological tissues and the biosensor. It should be noted that the yield of fluorescence depends on a number of parameters, of which the basic ones are the spatial distribution of fluorophores in the medium and their photophysical characteristics such as quantum yield, decay time, and some others [5].

Various theoretical models have been proposed for the description of excitation and propagation of fluorescence radiation in biological tissues. Among them are models based on electromagnetic theory [6, 7], the Kubelka–Munk approximation [8], diffusion theory [9], the theory of random walks [10], and numerical simulation by the Monte Carlo method [10–16]. A significant drawback of these studies is the initial assumption that the spatial distribution of fluorophores is homogeneous, whereas the results of numerous studies show that the distribution of fluorophores in skin tissues is highly inhomogeneous [12, 17, 18].

In this study, we present a model that makes it possible to describe the spatial distribution of fluorophores in human skin tissues and evaluate the localization of a detected fluorescence signal (the effective measurement region) corresponding to this distribution. The spatial distribution of fluorescence centers (fluorophores) in the medium is assumed to closely follow the spatial distribution of collagen fibers of the skin. Furthermore, in this work, particular attention is given to studying the possibility of increasing the contrast and degree of spatial localization of a detected signal. In our opinion, the optimal method for evaluating the spatial distribution of fluorescence sources and the region of localization of a detected signal is the Monte Carlo method [19–23]. In this study, we employ an improved algorithm specially developed for modeling fluorescence of biological tissues and evaluating the region of its localization. The general approach to the modeling of the propagation of incident optical (primary) and fluorescence radiation in biological tissues is described in the second part of the work. Then, the results of calculations of the spatial distribution of fluorescence sources and the effective measurement region corresponding to them are presented. In the last part of the work, conclusions and comments are given.

2. METHOD OF MODELING

The general scheme of modeling used in this study involves the description of processes of propagation of optical and fluorescence radiation in biological tissues, namely, the propagation of photons of exciting (primary) radiation to a point of absorption by a chromophore of a medium, the emission of a photon of fluorescence under the condition that the absorbing chromophore fluoresces, and the propagation of the photon of fluorescence to a point of exit from the medium in the detection region. The propagation of primary radiation in human skin, which is a multilayer randomly inhomogeneous medium strongly scattering and absorbing light, was modeled by the Monte Carlo method. This method combines schemes of calculation of genuine trajectories and the use of statistical weights [19, 20]. In the context of this modeling, particular features of propagation of photons in a medium determine such macroscopic parameters of the medium as the scattering coefficient μ_s, anisotropy factor g, absorption coefficient μ_a, and refractive index n. The path length of a photon packet l_i between successive scattering events is determined according to the probability density function $p(l_i) = \mu_t \exp(-\mu_t l_i)$ as [24]

$$l_i = -\frac{\ln \xi}{\mu_t}, \quad (1)$$

where μ_t is the coefficient of extinction of a layer of the medium ($\mu_t = \mu_s + \mu_a$) and ξ is a random number evenly distributed between 0 and 1. A new direction of propagation of the photon packet is chosen after each new scattering event according to the Henyey–Greenstein phase function with regard to the anisotropy of scattering [25].

The probability of reflection or refraction of the photon packet at an interface between layers of the medium or at its outer boundary is determined by the Fresnel formulas [26]. In this case, after each reflection or refraction at the outer boundary of the medium, the statistical weight W of the photon packet changes. According to [23], W is expressed as

$$W = [1 - R(\theta_i)][1 - R_{in}(\theta_i)]\left[\prod_{p=1}^{M-1} R(\theta_i)\right] W_0. \quad (2)$$

Here, $R_{in}(\theta_i)$ is determined by the reflection coefficient, which takes into account the initial reflection at the air–medium boundary; $R(\theta_i)$ is the Fresnel reflection coefficient; θ_i is the angle of incidence of the photon packet on the interface between layers of the medium; M is the number of events of interaction (reflection and/or refraction) of the photon packet at the outer boundary of the medium; and W_0 is the initial statistical weight of the photon packet. It was shown in [23] that such a representation allows one to adequately take into account partial and/or total internal reflection at the interfaces of the medium. The modeling of the propagation of the photon packet is terminated if the statistical weight of the packet becomes less than the minimum possible weight (10^{-4}) or if the number of scattering events experienced by the packet exceeds the specified maximum number (10^4). Outside these limitations, the contribution of any packet is assumed to be insignificantly small [23]. The absorption of the medium is taken into account using the modified Bouguer–Lambert–Beer law [27], according to which the statistical weight of a photon packet reaching a detector is calculated as

$$W(\mathbf{r}) = W_j \exp\left[-\sum_{i=1}^{N_j} \mu_a(\mathbf{r}) l_i\right]. \quad (3)$$

Here, N_j is the number of scattering events experienced by the photon packet in the course of its random walk; W_j is the statistical weight of the jth photon packet (2) reaching the detection region in the absence of absorption; and $\mu_a(\mathbf{r})$ is the absorption coefficient in an elementary volume of the medium with the center at point $\mathbf{r}$.

The process of modeling of fluorescence is shown schematically in Fig. 1. The probability of a fluorescence event at the ith step is defined as

$$W_{em}(\mathbf{r}) = W(\mathbf{r}) P_a P_\rho P_\gamma, \quad (4)$$

where P_a is the probability of fluorescence absorption of the photon packet in a given layer of the medium, P_ρ is the probability of absorption of photons by a given fluorophore (this probability depends on the concentration of the fluorophore and its spatial distribution), P_γ is the probability of the radiative transition of the fluoro-

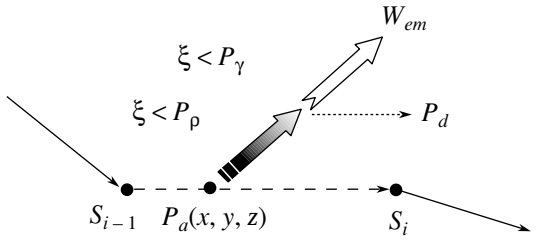

Fig. 1. Schematic representation of the fluorescence modeling. W_{em} is the probability of emission of fluorescence; P_a is the probability of absorption of a photon packet in a given layer of a medium; P_ρ is the probability of absorption of photons directly by a sensor fluorophore or collagen in dermal layers of skin; P_γ is the probability of a radiative transition of a fluorophore from an excited state, determined by the quantum yield γ; P_d is the probability of nonradiative processes, including phosphorescence and inelastic scattering events; and $\rho(x, y, z)$ is the spatial distribution of fluorophores in the dermis, which determines the coordinates of the fluorescence sources x, y, and z.

phore from an excited state to the ground state (this quantity is determined by the quantum yield γ), and $W(\mathbf{r})$ is the probability that the photon packet of the primary radiation reaches the point $\mathbf{r}(x, y, z)$ of the medium. Accordingly, $P_d = (1 - P_\gamma)$ determines the probability of dissipation caused by nonradiative processes, phosphorescence, and inelastic scattering, which accompany the absorption of photons by chromophores of the medium.

The spatial distribution of fluorophores in human skin tissues is highly inhomogeneous [12, 18, 28–30]. Thus, in the dermal layers of the skin, the main fluorophore is collagen, whose long fibers form a quasi-periodic lattice with diamond-shaped cells, with their characteristic size varying within 1–40 μm [31–33]. As the simplest model describing the packing of collagen fibers in the dermal layers, the following distribution was chosen:

$$\rho(\mathbf{r}) = \cos(kr_{x,y})\cos(kz), \qquad (5)$$

where $k = \pi/d$; d is the average diameter of the collagen fibers; and $r_{x,y} = r(x, y)$ and z are the coordinates of their location in the model medium. The distribution of fluorophores in the remaining layers (i.e., stratum corneum, epidermis, and subcutaneous fat) was assumed to be homogeneous. Therefore, the spatial distribution of the fluorescence sources is determined by the set of the coordinates of fluorescence centers $\mathbf{r}(x, y, z)$ and the probability of emission of fluorescence radiation at a given point of the medium $W_{em}(\mathbf{r})$. This modeling scheme makes it possible to consider the complex and inhomogeneous character of the distribution of fluorophores in the medium, their concentration, and the quantum yield.

Unlike the models in [14–16], in which the fluorescence radiation is isotropic and can only be emitted from scattering centers, in our model, the location of the sources of fluorescence is chosen randomly in accordance with the spatial distribution of fluorophores (Fig. 1). Following [10–16], we will use an isotropic angular distribution of fluorescence sources, assuming that the fluorescence is independent of the polarization of the exciting radiation. Furthermore, we will assume that the spectra of absorption and excitation of fluorophores do not overlap, which makes it possible to disregard the phenomenon of secondary fluorescence [5].

The effective region of measurements characterizing the spatial distribution of the specific flux of detected radiation is defined as the gradient of the intensity of fluorescence radiation with respect to the absorption coefficient (at the wavelength of fluorescence) in some elementary volume of a medium centered at a point $\mathbf{r}$ [19, 21]:

$$Q(\mathbf{r}) = -\frac{\partial}{\partial\mu_a(\mathbf{r})}\ln(I/I_0) = \sum_{j=1}^{M} l_j(\mathbf{r})W'_j/l_0\sum_{j=1}^{M} W'_j. \qquad (6)$$

Here, W'_j is the final statistical weight of the photon packet of fluorescence reaching the detection region provided that the initial weight of the packet is equal to W_{em}; M is the total number of detected photon packets; $l_j(\mathbf{r})$ is the total path length of a photon in an arbitrary elementary volume of the medium (which measures $10 \times 10 \times 10$ μm) centered at the point $\mathbf{r}$; and l_0 is the length of the edge of the unit cell. Below, we present the results of modeling of the effective region of measurements in the form of a profile of its spatial distribution $Q(\mathbf{r})$ over the depth $Q(z)$.

3. RESULTS OF MODELING

The algorithm described above was applied for estimating the spatial distribution of autofluorescence of skin tissues and fluorescence of a sensor layer—a "tattoo." The optical properties of the sensor layer used in modeling were chosen to be close to the properties of fluorescein, frequently used in various diagnostic applications [5, 34]. The optical properties of other layers of the medium, corresponding to the optical properties of normal skin in the blue-green spectral region at a wavelength of 488 nm [25, 28, 35, 36], are presented in the table. The selection of this wavelength for the fluorescence excitation is explained by its closeness to the maximum of absorption of fluorescein (494 nm) [34]. The differences between the optical properties at the fluorescence excitation wavelength and at the wavelength of propagation of the fluorescence radiation were considered to be insignificant. The thickness of the sensor layer t (the tattoo), occupying a part of the epidermis (the depth of location is 100 μm), was chosen to be equal to 50 μm, with the thickness of the epider-

Optical properties of skin layers and the biosensor

Skin layer	μ_s, mm^{-1}	μ_a, mm^{-1}	g	n	t, μm	d, μm	γ
Stratum corneum	40	0.2	0.9	1.5	20	–	0.01
Epidermis	35	0.15	0.85	1.34	80	–	0.01
Sensor layer	35	0.1	0.6	1.37	50	–	0.5
Papillary dermis	30	0.7	0.8	1.4	100	3	0.15
Superficial dermal plexus	35	1.0	0.9	1.39	80	6	0.15
Dermis	27	0.7	0.76	1.4	1500	20	0.15
Deep dermal plexus	35	1.0	0.95	1.39	200	30	0.15
Subcutaneous fat	15	0.3	0.8	1.44	5000	–	0.001

Note: The data were taken from [25, 35, 36].

mis itself being assumed to be 80 μm (table). The diameter of a source of primary optical radiation was chosen to be 200 μm, and the diameter of a detector, 1000 μm.

The results of modeling presented in Fig. 2 exhibit the presence of a clearly pronounced periodic structure in the spatial distribution of excited fluorescence of dermal layers. In the layer of the papillary dermis, at a depth of 150–250 μm, the periodicity in the distribution of fluorescence sources is less pronounced due to a small diameter of collagen fibers (0.3–3 μm) [31–33]. It should also be noted that the probability of fluorescence in the dermal layers is considerably higher than in the stratum corneum and epidermis, which agrees well with the experimental results [12, 18, 28]. However, the intensities of the sources of autofluorescence of the dermal layers (150–330 μm) and fluorescence of the sensor layer (100–150 μm) are in this case comparable with each other (Fig. 2).

Despite the complex inhomogeneous character of the distribution of fluorescence sources in the medium (Fig. 2), the distribution of the detected fluorescence signal proved to be rather homogeneous with a clearly pronounced maximum in the sensor and upper dermal layers, although the contribution from such near-surface skin layers as the stratum corneum and epidermis is also considerable (Fig. 3). The results obtained clearly illustrate the necessity of further analysis of the detected signal in terms of its quantitative interpretation and determination of partial contributions from the sensor and dermal layers. Note also that the near-surface skin layers, most strongly scattering light, in combination with the difference in the refractive indices of the layers (1 : 1.5 : 1.34) produce a sort of screening effect upon input and output of sounding radiation [21, 23, 37], which is highly undesirable. It is shown that the spatial localization and contrast can be significantly improved by equalizing the refractive indices of the surrounding medium and the medium to be sounded (Fig. 3). The equalizing of the refractive indices strongly reduces (up to zero) the Fresnel reflection at the external medium–skin interface, which, in turn, leads to a decrease in the contribution from surface layers (the stratum corneum and epidermis) to the detected fluorescence signal. In this case, beginning from the sensor layer, the effective measurement region is virtually evenly distributed over the depth down to the sanguiferous dermal layers.

The equalizing of the refractive indices at the interface between the media can be realized by using special liquids or gels equalizing the refractive indices of the stratum corneum and an adjacent medium between the surface of the medium and the detector. It should also be noted that, evidently, the highest efficiency of the method presented could be achieved in combination with the immersion method, whose application notice-

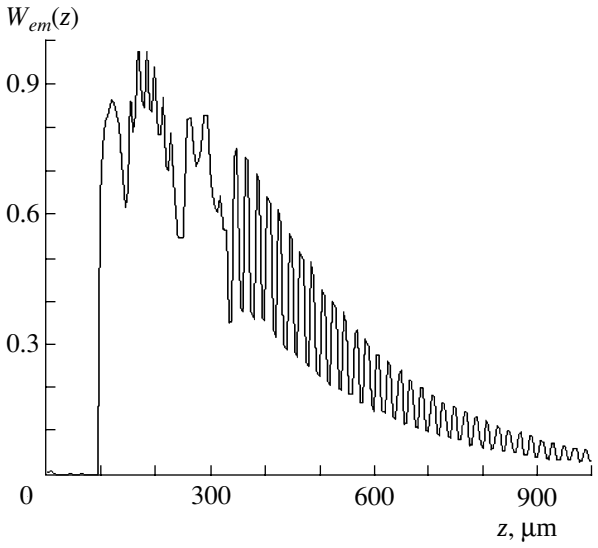

Fig. 2. The spatial distribution of fluorescence sources in skin tissues $W_{em}(z)$. The relevant optical properties of the skin layers corresponding to the radiation wavelength 488 nm are listed in the table. The geometrical parameters of the radiation source are as follows: the diameter is 200 μm and the numerical aperture is 0.63 (the maximum admissible angle of the input and detection of radiation amounts to 40°). The refractive index of the surrounding medium n_0 is equal to 1.

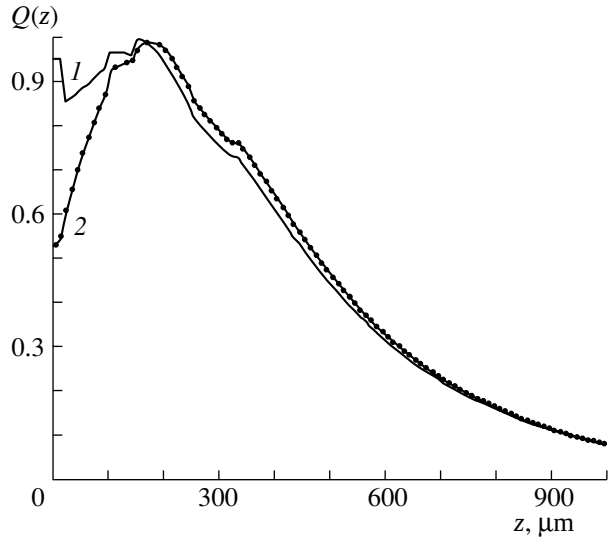

Fig. 3. The spatial distribution of the effective detection region $Q(z)$: (*1*) the refractive indices of the stratum corneum ($n = 1.5$) and external medium ($n_0 = 1$) are different; (*2*) the refractive indices of the stratum corneum and external medium are equal ($n = n_0 = 1.5$). The relevant optical properties of the skin layers corresponding to the radiation wavelength 488 nm are listed in the table. The diameter of the source is equal to 200 μm; the diameter of the detector is equal to 1000 μm. The numerical apertures of the source and detector amount to 0.63. In the case of equality of the refractive indices, the maximum admissible angle of the input and detection of radiation amounts to 25°.

ably improves the spatial localization of the detected signal [21, 22, 38].

4. CONCLUSIONS

In this study, we presented a new improved model for and results of modeling of fluorescence of skin tissues and a sensor layer—a tattoo—located at the depth of the dermal–epidermal interface. This model takes into account the inhomogeneous spatial distribution of fluorophores in biological tissues, their concentration, and the quantum yield. The model distribution of fluorescence sources in dermal layers forms an inhomogeneous periodic structure, which agrees with experimental observations of autofluorescence of skin samples. Our calculations, aimed at estimating the efficiency of a fluorescence signal detected in the range of the sensor location, show that the equalizing of the refractive indices of the surrounding medium and the stratum corneum markedly reduces the contribution of the surface skin layers to the detected signal and enhances the contrast in the spatial localization of this signal in the range of the sensor (the tattoo). At the same time, the total contribution of the sensor and the upper dermal layers to the detected fluorescence signal remains unchanged.

The method presented can be recommended for quantitative estimation of the efficiency of various optical measuring systems used in experimental biomedical fluorescence spectroscopy. In addition, a potential area of application of this model of fluorescence could be two-photon fluorescence microscopy.

ACKNOWLEDGMENTS

We are grateful to V.V. Tuchin, Yu.P. Sinichkin, M.C. Jermy, and A.N. Bashkatov for valuable advice and remarks.

REFERENCES

1. A. DeMaria, OE Mag. **3** (5), 4 (2003).
2. P. R. Coulet and A. P. F. Turner, in *Biosensor Principles and Applications*, Ed. by L. J. Blum and P. R. Coulet (Marcel Dekker, New York, 2001), p. 7.
3. A. J. Cunningham, *Introduction to Bioanalytical Sensors* (Wiley, New York, 1998).
4. I. V. Meglinski, S. A. Piletsky, D. A. Greenhalgh, and A. P. F. Turner, in *Proceedings of Second International Workshop on Molecularly Imprinted Polymers* (La Grande Motte, France, 2002), p. 55.
5. J. R. Lakowicz, *Principles of Fluorescence Spectroscopy* (Plenum, New York, 1983; Mir, Moscow, 1986).
6. O. Panou-Diamandi, N. K. Uzunoglu, G. Zacharakis, *et al.*, J. Electromagn. Waves **12**, 1101 (1998).
7. A. J. Durkin, S. Jaikumar, N. Ramanujam, and R. Richards-Kortum, Appl. Opt. **33**, 414 (1994).
8. M. S. Patterson and B. W. Pogue, Appl. Opt. **33**, 1963 (1994).
9. A. H. Gandjbakhche, R. F. Bonner, R. Nossal, and G. H. Weiss, Appl. Opt. **36**, 4613 (1997).
10. R. Richards-Kortum, in *Optical–Thermal Response of Laser Irradiate Tissue*, Ed. by A. J. Welch and M. J. C. Van Gemert (Plenum, New York, 1995), p. 667.
11. R. J. Crilly, W. F. Cheong, B. Wilson, and J. R. Spears, Appl. Opt. **36**, 6513 (1997).
12. H. Zeng, C. McAulay, D. I. McLean, and B. Palcic, J. Photochem. Photobiol., B **38** (3), 234 (1997).
13. A. J. Welch, C. Gardner, R. Richards-Kortum, *et al.*, Lasers Surg. Med. **21**, 166 (1997).
14. M. J. McShane, S. Rastegar, M. Pishko, and G. L. Cote, IEEE Trans. Biomed. Eng. **47**, 624 (2000).
15. B. Pogue and G. Burke, Appl. Opt. **37**, 7429 (1998).
16. K. Vishwanath, B. Pogue, and M. A. Mycek, Phys. Med. Biol. **47**, 3387 (2002).
17. Y. P. Sinichkin, S. R. Utz, I. V. Meglinskiĭ, and E. A. Pilipenko, Opt. Spektrosk. **80**, 431 (1996) [Opt. Spectrosc. **80**, 383 (1996)].
18. H. Zeng, C. McAulay, D. I. McLean, and B. Palcic, Photochem. Photobiol. **61**, 639 (1995).
19. I. V. Meglinsky and S. J. Matcher, Med. Biol. Eng. Comput. **39**, 44 (2001).
20. I. V. Meglinskiĭ and S. D. Matcher, Opt. Spektrosk. **91**, 692 (2001) [Opt. Spectrosc. **91**, 654 (2001)].
21. I. V. Meglinskiĭ, A. N. Bashkatov, É. A. Genina, *et al.*, Kvantovaya Élektron. (Moscow) **32**, 875 (2002).
22. I. V. Meglinski, A. N. Bashkatov, E. A. Genina, *et al.*, Laser Phys. **13**, 65 (2003).

23. D. Y. Churmakov, I. V. Meglinski, and D. A. Greenhalgh, Phys. Med. Biol. **47**, 4271 (2002).
24. I. M. Sobol', *The Monte-Carlo Method* (Nauka, Moscow, 1985).
25. V. V. Tuchin, *Lasers and Fiber Optics in Biomedical Investigations* (Sarat. Gos. Univ., Saratov, 1998).
26. M. Born and E. Wolf, *Principles of Optics*, 7th ed. (Cambridge Univ. Press, Cambridge, 1999; Nauka, Moscow, 1973).
27. D. T. Delpy, M. Cope, P. Van der Zee, *et al.*, Phys. Med. Biol. **33**, 1433 (1988).
28. Yu. P. Sinichkin and S. R. Utts, *In vivo Reflected and Fluorescent Spectroscopy of the Human Skin* (Sarat. Gos. Univ., Saratov, 2001).
29. Y. P. Sinichkin, N. Kollias, G. I. Zonios, *et al.*, in *Handbook of Optical Biomedical Diagnostics*, Ed. by V. V. Tuchin (SPIE Press, Washington, 2002), Vol. PM107, p. 727.
30. A. R. Young, Phys. Med. Biol. **42**, 789 (1997).
31. L. T. Smith, K. A. Holbrook, and P. H. Byers, J. Invest. Dermatol. **79** (Suppl. 1), S93 (1982).
32. G. F. Odland, in *Physiology, Biochemistry and Molecular Biology of the Skin*, Ed. by L. A. Goldsmith (Oxford Univ. Press, Oxford, 1991), Vol. 1, p. 3.
33. W. Montagna, A. M. Kligman, and K. S. Carlisle, *Atlas of Normal Human Skin* (Springer, New York, 1992).
34. H. Schneckenburger, K. Stock, R. Steiner, *et al.*, in *Handbook of Optical Biomedical Diagnostics*, Ed. by V. V. Tuchin (SPIE Press, Washington, 2002), Vol. PM107, p. 825.
35. W. F. Cheong, S. A. Prahl, and A. J. Welch, IEEE J. Quantum Electron. **26**, 2166 (1990).
36. M. J. C. van Gemert, S. L. Jacques, H. J. C. M. Sterenborg, and W. M. Star, IEEE Trans. Biomed. Eng. **36**, 1146 (1989).
37. D. Sliney and M. Wolbarsht, *Safety with Lasers and Other Optical Sources. A Comprehensive Handbook* (Plenum, New York, 1980).
38. R. K. Wang, X. Xu, V. V. Tuchin, and J. B. Elder, J. Opt. Soc. Am. B **18**, 948 (2001).